KEEP THIS COPY FOR REPRODUCTION PURPOSES

REPORT

Form Approved
OMB No. 0704-0188

1. AGENCY USE ONLY (Leave blank)	2. REPORT DATE	T TYPE AND DATES COVERED
	6/17/94	

4. TITLE AND SUBTITLE

"Quantum Transport in Semiconductor Devices"

5. FUNDING NUMBERS

DAAL03-91-G-0067

6. AUTHOR(S)

David K. Ferry

7. PERFORMING ORGANIZATION NAME(S) AND ADDRESS(ES)

Arizona State University
Center for Solid State Electronics Research
Tempe, AZ 85287-6206

8. PERFORMING ORGANIZATION REPORT NUMBER

9. SPONSORING/MONITORING AGENCY NAME(S) AND ADDRESS(ES)

U. S. Army Research Office
P. O. Box 12211
Research Triangle Park, NC 27709-2211

10. SPONSORING/MONITORING AGENCY REPORT NUMBER

ARO 28461.11-EL

11. SUPPLEMENTARY NOTES

The view, opinions and/or findings contained in this report are those of the author(s) and should not be construed as an official Department of the Army position, policy, or decision, unless so designated by other documentation.

12a. DISTRIBUTION/AVAILABILITY STATEMENT

Approved for public release; distribution unlimited.

12b. DISTRIBUTION CODE

13. ABSTRACT *(Maximum 200 words)*

This program concentrated on research investigating quantum effects which become important in ultra-small semiconductor devices, and the manner in which these effects may limit downscaling of individual feature sizes. The major concentrations of the program were on:

1. Tunneling in gated semiconductor structures, an effect which has been found to be important in normal high-electron mobility transistors (HEMTs) with gate lengths of $\leq 0.025\mu m$.
2. The role played by slab and interface phonon modes in transport within small semiconductor devices.
3. Modeling of quantum effects in MESFET devices as a general tool for approaching the inclusion of such effects in dynamic semiconductor device models.

14. SUBJECT TERMS

Semiconductor Devices; Hydrodynamic Equations; Velocity Overshoot; MESFETs; Device Modeling

15. NUMBER OF PAGES

18

16. PRICE CODE

17. SECURITY CLASSIFICATION OF REPORT	18. SECURITY CLASSIFICATION OF THIS PAGE	19. SECURITY CLASSIFICATION OF ABSTRACT	20. LIMITATION OF ABSTRACT
UNCLASSIFIED	UNCLASSIFIED	UNCLASSIFIED	UL

QUANTUM TRANSPORT IN SEMICONDUCTOR DEVICES

Final Report on DAAL03-91-G-0067 (28461-EL)

David K. Ferry, Principal Investigator

Department of Electrical Engineering
Arizona State University
Tempe, Arizona 85287-5706

June 30, 1994

CONTENTS

I. PUBLICATIONS UNDER THIS GRANT

1. J.-R. Zhou and D. K. Ferry, "Simulation of Ultra-Small GaAs MESFETs Using the Quantum Moment Equations," Semiconductor Science and Technology **7**, B546-B548 (1992).

2. H. L. Grubin, T. R. Govindan, B. J. Morrison, D. K. Ferry, and M. A. Stroscio, "Temperature Description of Transport in Single- and Multiple-Barrier Tunneling Structures," Semiconductor Science and Technology **7**, B360-B363 (1992).

3. J.-R. Zhou and D. K. Ferry, "Simulation of Ultra-Small GaAs MESFETs Using Quantum Moment Equations," IEEE Transactions on Electron Devices **39**, 473-8 (1992).

4. J.-R. Zhou and D. K. Ferry, "Simulation of Ultra-Small GaAs MESFETs Using Quantum Moment Equations: II. Velocity Overshoot," IEEE Trans. Electron Dev. **39**, 1793-1796 (1992).

5. J.-R. Zhou and D. K. Ferry, "Modeling of quantum effects in ultrasmall HEMT devices," IEEE Trans. Electron Dev. **40**, 421-427 (1993).

6. K. Tsukioka, D. Vasileska, and D. K. Ferry, "Ensemble Monte Carlo Studies of High-Field Transport in b-SiC," Physica B **185**, 466-470 (1993).

7. J. M. Ryan, N. F. Deutscher, and D. K. Ferry, "Edge-State Tunneling through Ultra-Short Gates," Physical Review B **47**, 16594 (1993).

8. J.-R. Zhou, D. Vasileska, and D. K. Ferry, "Modeling of b-SiC MESFETs Using Hydrodynamic Equations," Solid-State Electronics **36**, 1289 (1993).

9. D. K. Ferry and J.-R. Zhou, "On the Form of the Quantum Potential for Use in Hydrodynamic Equations for Semiconductor Device Modeling," Physical Review B **48**, 7944 (1993).

10. J. M. Ryan, N. F. Deutscher, and D. K. Ferry, "Gated-Region Transport in the Quantum Hall Effect," Physical Review B**48**, 8840 (1993).

11. T. Yamada, H. Miyata, J.-R. Zhou, and D. K. Ferry, "Monte Carlo Study of Low Temperature Mobility of Electrons in a Strained Si Layer Grown on a $Si_{1-x}Ge_x$ Substrate," Physical Review B **49**, 1875-81 (1994).

12. D. K. Ferry, "Future Ultra-Large Scale Integration: Transport Physics in Semiconductor Nanostructures," Japanese Journal of Applied Physics **33**, 873-878 (1994).

13. T. Yamada, J.-R. Zhou, H. Miyata, and D. K. Ferry, "Velocity Overshoot in a Modulation Doped $Si/Si_{1-x}Ge_x$ Structure," Semiconductor Sci. Technol. **9**, 775 (1994).

14. H. L. Grubin, J. P. Kreskovsky, T. R. Govindan, and D. K. Ferry, "Use of the Quantum Potential in Modeling Hot Carrier Semiconductor Devices," Semiconductor Sci. Technol. **9**, 855 (1994).

15. D. K. Ferry, "A Perspective on Nanodevices," Proceedings of the MicroProcess Conference, Kanazawa, Japan, 15-18 July 1991; Jpn. J. Appl. Phys Series 5, 335-341 (1991).

16. J.-R. Zhou and D. K. Ferry, "Modeling of Quantum Barrier Devices Using Quantum Moment Equations," Proc. of the International Workshop on Computational Electronics, Urbana, IL, May 28-29, 1992, 167-170.

17. D. K. Ferry and H. L. Grubin, "Techniques for Modeling Ultrasmall Quantum Devices," Proc. Workshop on Computational Electronics, Leeds, 1993 (Invited).

18. J.-R. Zhou, T. Yamada, H. Miyata, and D. K. Ferry, "Simulation of a Si/SiGe Modulation-Doped FET Using Quantum Hydrodynamic Equations," Proc. Workshop on Computational Electronics, Leeds, 1993.

19. D. K. Ferry, "Transport Physics in Semiconductor Nanostructures," Proc. 1993 Intern. Conf. on Solid State Devices and Materials (Ctr. for Academic Societies, Tokyo, 1993) (Invited) 312-314.

20. Jing-Rong Zhou and D. K. Ferry, "2-D Simulation of Quantum Effects in Small Semiconductor Devices Using Quantum Hydrodynamic Equations," VLSI, in press.

21. T. Yamada, J.-R. Zhou, H. Miyata, and D. K. Ferry, "In-Plane Transport Properties of $Si/Si_{1-x}Ge_x$ Structure and Its FET Performance by Computer Simulation," IEEE Trans. Electron Devices, in press.

22. N. F. Deutscher, J. M. Ryan, and D. K. Ferry, "Gated Non-Local Magnetoresistance Measurements in GaAs/AlGaAs Heterostructure," Semiconductor Sci. Technol., in press.

23. D. Vasileska-Kafedziska, P. Bordone, and D. K. Ferry, "The Effect of Interface-Roughness on the Conductivity in Quantum Wells at Zero-Temperature," Physical Review B, in press.

24. J.-R. Zhou and D. K. Ferry, "Three-Dimensional Simulation of the Effect of Random Impurity Distributions on Conductance for Deep Submicron Devices," submitted for publication.

25. D. Vasileska-Kafedziska, P. Bordone, and D. K. Ferry, "The Analytical Derivation of the Conductivity in Low-Dimensional Systems Using a Real-Time Green's Function Formalism," submitted for publication.

26. N. F. Deutscher and D. K. Ferry, "Nonlocal Universal Conductance Fluctuations in a GaAs/AlGaAs Heterostructure," submitted for publication.

II. PERSONNEL SUPPORTED UNDER THIS GRANT

Faculty:

Dr. David K. Ferry, Principal Investigator

Research Staff:

Dr. Jing-Rong Zhou (Received Ph. D. on this, and earlier ARO grant in 1991).

Students:

Thomas Rössler (dropped out of program)

Dragica Vasileska-Kafediska (currently a doctoral student)

Neil Deutscher (received Ph. D. May 1994)

Cherng-Nan Tang (recieved M.S. May 1992, currently in Singapore)

III. Green's Function Formalism For Low-Dimensional Systems, *Dragica Vasileska-Kafedziska and Paolo Bordone.* We present an analytical derivation of the one-electron Green's function in quantum wells, with both impurities and rough surfaces, using a zero-temperature Green's function formalism. We also give the numerical results for the density of states (DOS) function and conductivity for the case with an idealy flat interface only. The numerical simulation of surface-roughness are still in progress. The transport properties of low-dimensional systems have been the focus of scientific research for many years, but more so recently due to advances in microfabrication of metallic and semiconductor nanostructures.[1] In these systems, the width of the channel becomes comparable to the de Broglie wavelength and therefore, the motion of the electrons in the direction perpendicular to the interface is no longer free. The energy levels of the electrons are grouped into electronic sub-bands, each of which corresponds to the particular quantized level for transverse motion. The electrons are free to move in the plane parallel to the interface.

At low temperatures, the dominant scattering mechanisms in these structures are impurities and surface roughness.[2] The effect of impurities on the conductivity in low-dimensional systems has been analyzed using the Green's function approach.[3-5] In thin quantum wells, only a small roughness of the heterointerface can cause a large fluctuation in the quantization energy of confined Q2D-electrons, which could lead to a signifficant momentum scattering. Therefore, for small channel widths, the effect of the rough boundaries dominates the transport properties of the electrons.[6] Early theories were based on the Boltzmann equation in which the surface is incorporated via boundary conditions on the electron distribution function.[7-9] The first quantum-mechanical treatment of the problem was given by Prange and Nee.[10]

We consider a model for a spin 1/2 Q2D-electron gas with a square-well confinement potential in the z-direction as shown in Fig.1. The states of the quantum well are considered to be area-normalized plane waves in the directions along the well, and to be describable in

terms of the wave functions for an infinitely deep well in the directions normal to the interfaces.

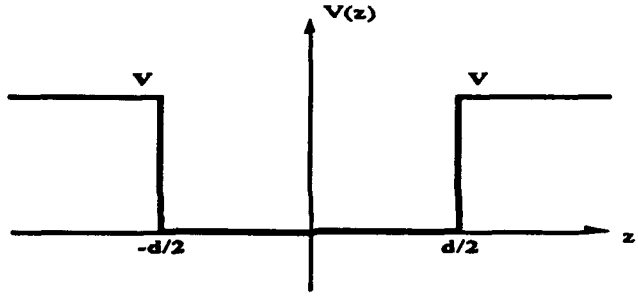

Fig.1 Potential energy profile of the quantum well structure

The first quantized form of the perturbing part of the Hamiltonian, due to impurities, is given by

$$H_{imp}(\mathbf{R}) = \sum_i u(\mathbf{r}-\mathbf{r}_i, z-z_i) = u\sum_{i,\mathbf{q}} e^{i\mathbf{q}(\mathbf{r}-\mathbf{r}_i)}\delta(z-z_i) \qquad (1)$$

The sum runs over all impurity positions. For simplicity, we have taken a δ-function impurity potential with strength u. Only the diagrams where we have multiple scattering from the same impurity are considered.

The effect of the surface roughness is treated through a perturbation term of the form:

$$H_{sr}(\mathbf{R}) = -Vf(\mathbf{r})\delta\left(z-\frac{1}{2}d\right), \qquad (2)$$

where $f(\mathbf{r})$ characterizes the change in the width of the well. The Hamiltonian $H_{sr}(\mathbf{R})$ gives the local fluctuations of the quantization energy of the electrons. These fluctuations work as a scattering potential for the 2D-electrons motion. The strength of the scattering potential is described with two fitting parameters: the height of the bumps Δ and the lateral size ζ of the assumed Gaussian fluctuations[11-15] of the interface, expressed through the autocorrelation function:

$$\langle f(\mathbf{r})f(\mathbf{r}')\rangle = \Delta^2 \exp\left(-\frac{|\mathbf{r}-\mathbf{r}'|^2}{\zeta^2}\right) = G_{sr}(|\mathbf{r}-\mathbf{r}'|), \qquad (3)$$

where < ... > means an ensemble average over different surfaces with different locations of the bumps. The Fourier transform of this autocorrelation function is:

$$G_{zz}(q) = \pi\zeta^2 \exp\left(-\frac{q^2\zeta^2}{4}\right) \tag{4}$$

The equation of motion for the unperturbed Green's function at zero temperature can be written in the general form

$$G_o(\mathbf{R},\mathbf{R}',t-t') = \sum_n \psi_n^*(z')\psi_n(z) g_{on}(\mathbf{r},\mathbf{r}',t-t') \tag{5}$$

since

$$\delta(z-z') = \sum_n \psi_n^*(z')\psi_n(z) \tag{6}$$

The full Green's function is calculated in the so-called damping theoretical approximation[16] (Fig. 2a). In this approximation the scattering mechanisms (impurities and surface-roughness) are taken into account in the lowest Born one, whereas the broadening effect is included self-consistently as shown in Fig.2(b-c). This is a very good approximation for the cases when the concentration of the scatterers is not too high. Assuming that the full Green's function is of the same form as the unperturbed one, we get that the Fourier transform of the subband Green's function equals to:

$$g_n(\mathbf{k},\omega) = \frac{1}{\hbar\omega - \varepsilon_k - \varepsilon_n - n_i u^2 \sum_m \sum_{\mathbf{q}} O_{nm} g_m(\mathbf{k}-\mathbf{q},\omega) - \frac{\hbar^4\pi^4 n^2 \Delta^2}{m^{*2} d^6} \sum_m \sum_{\mathbf{q}} m^2 G_{zz}(\mathbf{q}) g_m(\mathbf{k}-\mathbf{q},\omega)}, \tag{7}$$

where n_i is the impurity concentration and the overlap factors O_{nm} are defined by

$$O_{nm} = \int_{-d/2}^{d/2} dz \left|\psi_n(z)\right|^2 \left|\psi_m(z)\right|^2 \tag{8}$$

Since the retarded sub-band Green's function is always of the form

$$g_n^r(\mathbf{k},\omega) = \frac{1}{\hbar\omega - \varepsilon_{\mathbf{k}} - \varepsilon_n + R_n(\mathbf{k},\omega) + i\Gamma_n(\mathbf{k},\omega)}, \tag{9}$$

where $R_n(\mathbf{k},\omega)$ gives the shift in the sub-band energies, which is usually small and $\Gamma_n(\mathbf{k},\omega)$ is proportional to the inverse of the lifetime of the n-th state, substituting (9) into (7) gives

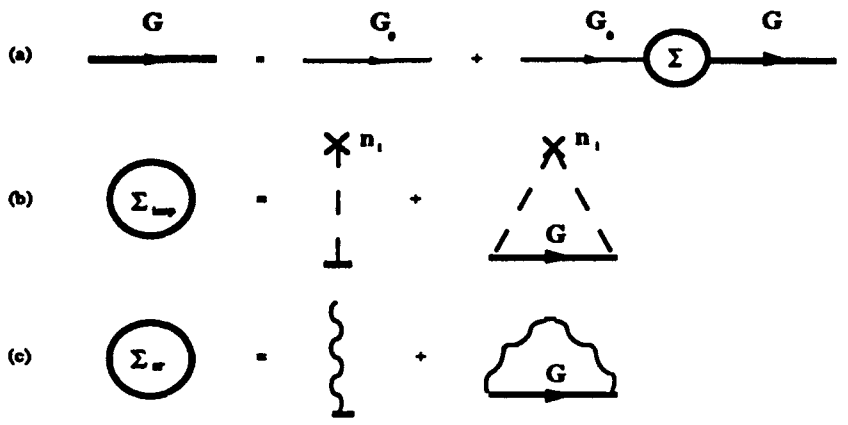

Fig. 2 Damping Theoretical approximation of the zero-temperature Green's function. (a) Dyson's equation, (b) Self-energy approximation for the scattering from impurities, (c) Self-energy approximation for surface-roughness scattering.

$$\begin{cases} R_n(\varepsilon_k,\omega) = c_{sr}\sum_m m^2 n^2 \int_0^{\infty} d\varepsilon_q \dfrac{\hbar\omega - \varepsilon_m - \varepsilon_q - R_m(\varepsilon_q,\omega)}{\left[\hbar\omega - \varepsilon_m - \varepsilon_q - R_m(\varepsilon_q,\omega)\right]^2 + \Gamma_m^2(\varepsilon_q,\omega)} I_0(2\alpha\sqrt{\varepsilon_k\varepsilon_q})\exp[-\alpha(\varepsilon_k+\varepsilon_q)] \\ \Gamma_n(\varepsilon_k,\omega) = \sum_m \int_0^{\infty} d\varepsilon_q \Gamma_m(\varepsilon_q,\omega) \dfrac{c_{imp}O_{nm} + c_{sr}n^2m^2 I_0(2\alpha\sqrt{\varepsilon_k\varepsilon_q})\exp[-\alpha(\varepsilon_k+\varepsilon_q)]}{\left[\hbar\omega - \varepsilon_m - \varepsilon_q - R_m(\varepsilon_q,\omega)\right]^2 + \Gamma_m^2(\varepsilon_q,\omega)} \end{cases}$$

where

$$\alpha = \frac{m^*\zeta^2}{2\hbar^2}, c_{imp} = \frac{n_i u^2 m^*}{2\pi\hbar^2}, c_{sr} = \frac{\hbar^2\pi^4\zeta^2\Delta^2}{2m^* d^6} \quad , \tag{11}$$

and I_0 is the modified Bessel function of the zero order. The coupled equations given in (10) need to be solved self-consistently. For idealy flat interfaces $\Gamma_n(\mathbf{k},\omega)$ does not depend upon the values of the **k**-vector. In this case, the perturbed DOS defined in analogy with the equations (15) and (16) can be approximated as

$$\rho(\omega) \approx \sum_n \frac{m^*}{\pi\hbar^2}\left[\frac{1}{2} + \frac{1}{\pi}\tan^{-1}\left(\frac{\hbar\omega - \varepsilon_n}{\Gamma_n}\right)\right] . \tag{12}$$

The Drude approximation for the conductivity in this particular case gives

$$\sigma(\omega) = \frac{e^2}{2\pi^2\hbar}\sum_n \frac{\hbar\omega - \varepsilon_n}{\Gamma_n}\left[\frac{\pi}{2} + \tan^{-1}\left(\frac{\hbar\omega - \varepsilon_n}{\Gamma_n}\right)\right] . \tag{13}$$

The normalized DOS for the first two subbands for the quantum well with idealy flat interfaces and impurity concentration $n_i = 5 \times 10^{16} cm^{-3}$ are shown in Fig. 3. The width of the well is 30 angstroms. Due to the quantum size effects, we see a noticable change in the shape of the DOS curve for energies close to the subband energies. The smoothening effect is more pronounced for higher subbands where the effect of the mixing of the bands is more important.

The Drude approximation for the conductivity vs the thickness of the well is given on Fig. 4. The parameter for this curve is the total energy of the electrons (1.5 eV). The dips in the conductivity curve appear when new subbands are populated. As can be seen from the figure, the depth of the dips is lower for wider wells where the number of populated subbands is large. These dips would be further hidden by temperature broadening effects which are not considered here.

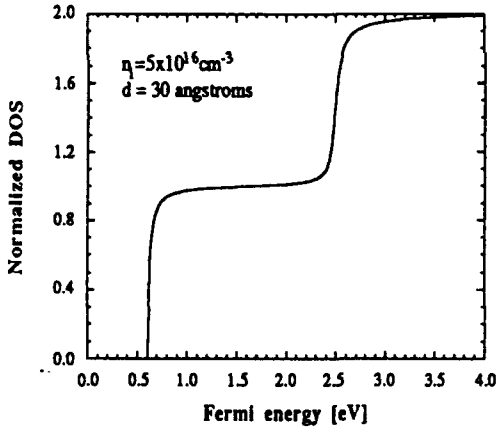

Fig.3 Normalized DOS vs Fermi energy for quantum well with idealy flat interfaces

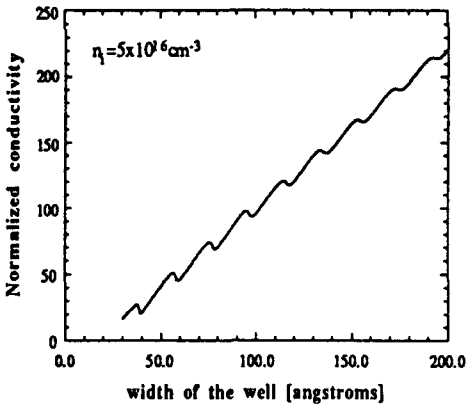

Fig.4 The variation of the conductivity with the width of the well

References

1. T. Ando, A. B. Fowler, and F. Stern, Rev. Mod. Phys. **54**, 437 (1982)
2. T. Ando and Y. Uemura, J. Phys. Soc. Jpn. **36**, April 1974.
3. D. G. Cantrell, P. N. Butcher, Solid State Phys. **18**, 5111 (1985).

4. M. J. Kearner, P. N. Butcher, Solid State Phys. **20**, 47 (1987).

5. M. Suhrke, S. Wilke and R. Keifer, J. Phys. Cond. Matter **2**, 6743 (1990).

6. H. Sakaki, T. Noda, K. Hirakowa, M. Tanaka and T. Matsume: Appl. Phys. Lett. **51**, 1934 (1987).

7. J. J. Thomson, Proc. Cambridge Philos. Soc. **11**, 1120 (1901).

8. K. Fuchs, Proc. Cambridge Philos. Soc. **34**, 100 (1938).

9. E. H. Sondheimer, Adv. Phys. **1**, 1 (1952).

10. E. Prange and T. Nee, Phys. Rev. **168**, 779 (1968).

11. S. M. Goodnick, R. G. Gann, D. K. Ferry and C. W. Wilmsen, Surface Science **113**, 233 (1982).

12. A. Gold, Solid State Commun. **60**, 531 (1986).

13. A. Gold, Phys. Rev. B **35**, 723 (1987).

14. G. Fishman and D. Calecki, Phys. Rev. Lett. **62**, 1302 (1989).

15. Y. C. Cheng, in Proc. 3rd Conf. on Solid State Devices, Tokyo, 1971 [Suppl. J. Japan. Soc. Appl. Phys. **1**, 173 (1972)].

16. J. M. Luttinger, in *Mathematical Methods in Solid State and Superfluid Theory*, Ed. by R. C. Clark and G. H. Derrick (Plenum Press, New York, 1967), p.157 .

IV. Simulation of Random Impurity Distribution Effect on Conductance Fluctuation for Deep Submicron Devices, ***Jing-Rong Zhou.*** As devices scale down to the deep submicron regime, especially for device feature size less than 0.1 μm, the active device region will contain so few dopant atoms that the statistical fluctuation of the dopants either in total number and/or in spatial distribution in the device may cause non-negligible effects on device performance. The anticipated effects include: 1) universal conductance fluctuation caused by quantum interference effect from electron waves propagating through the semiconductor [1]; 2) the device current level shift and threshold voltage shift due to the total dopant number fluctuation and/or distribution. The current research is devoted to better understanding these processes. We are carrying on simulations for 3-dimensional device structure of MESFETs and HEMTs by using Quantum Moment Equations, in which the discretized 3-dimensional random impurity distribution and fluctuation can be included.

The simulated device structure is a domain of 0.36 μm (L) × 0.1 μm (H) × 0.045 μm (W). The discrete impurity region is defined in the high-doped layer away from the simulation domain boundary in order to use the existing simulation program and avoid dealing with very complicated rough boundary conditions for the time being. This treatment should not affect the simulation results much since most of the active device region is covered by the discrete impurity distribution and device operation is dominated by the electron transport through the discrete impurity region. The doping in the high doped layer is 1.5×10^{18} cm^{-3} for a uniform doping. The total number of dopants in the discretized region is determined by taking the total charge in the region divided by a single ion charge. The distribution of the discretize charge in the discretized simulation cells is done by check the assigned random number in each cell by computer random number generator. When the random number for a cell is greater than one minus the ratio of the total number of dopants in the region to the total discretized cells in the region, the cell is assigned an ion charge. The

distributions for different devices generated by the procedure is similar to a physical device process such as ion-implantation. The simulation method is the same as we used in [2].

Fig. 1 shows the simulation results of AlGaAs/GaAs HEMTs, in which the drain current versus gate voltage characteristics is plotted. In this results, no clear conductance fluctuation is observed. This suggests that in this device size and simulation temperature (300 K), the quantum interference is still averaged out. Further investigation on the possible Universal Conductance Fluctuation need to be considered.

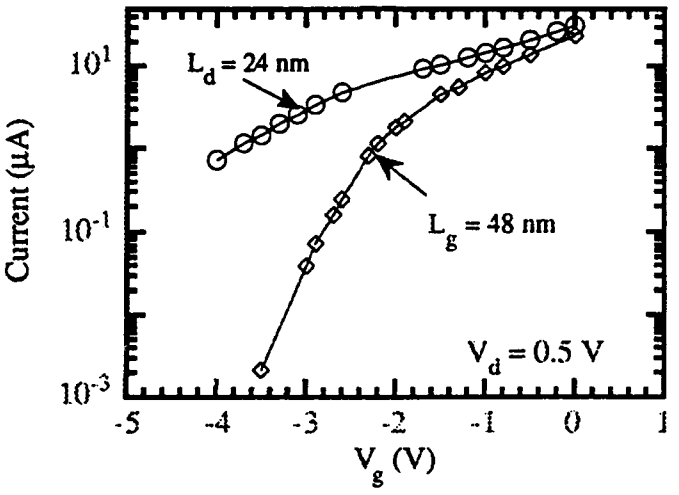

Fig. 1 The drain current vs gate voltage characteristics of HEMT devices with gate length of 24 nm and 48 nm, respectively. The drain potential is fixed at 0.5 V.

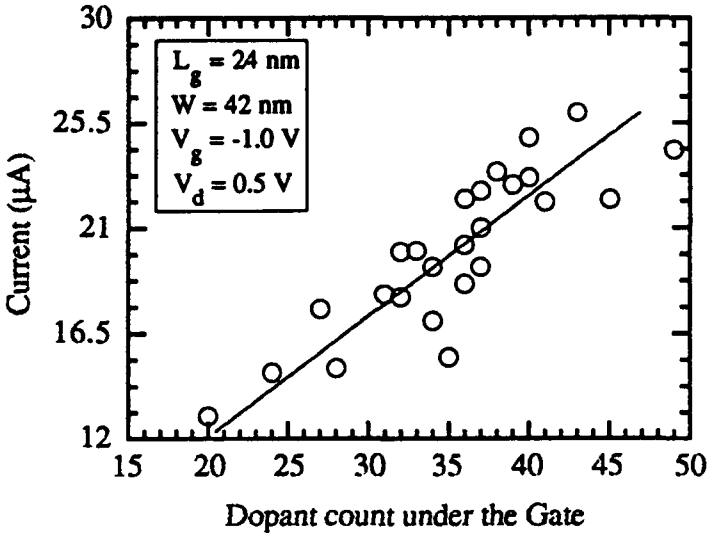

Fig. 2 Current fluctuation as a function of dopant number under the gate of GaAs MESFETs.

The study of the effect of random impurity distribution and fluctuation, however, predicts large current fluctuations. Fig. 2 illustrates the current fluctuation for 25 GaAs MESFET devices, with the same geometry, but different random impurity distributions in which the gate voltage is -1.0 V and the drain voltage is 0.5 V. Two characteristics are obvious: 1) the total dopant fluctuation under the gate causes current fluctuation. The current increases essentially with the increase of the dopant under the gate, which means that higher dopant concentration provides higher electron density in the channel and also wider channel opening since less depletion will occur with the same bias voltage; 2) Different dopant distributions cause current fluctuations. The current fluctuates even with the same total dopant number under the gate, which implies that different distribution can cause different potential fluctuation under the gate and results in stronger or weaker control of the channel current flow under the same bias condition. The simulation shows that the fluctuation can be as large as 50 per cent for this particular MESFET device structure. Figure 3 shows that the current fluctuation doesn't follow the total dopant fluctuation in the discrete dopant region

clearly. And Fig. 4 states that the total dopant number under the gate is not necessary following the total dopant number in the region.

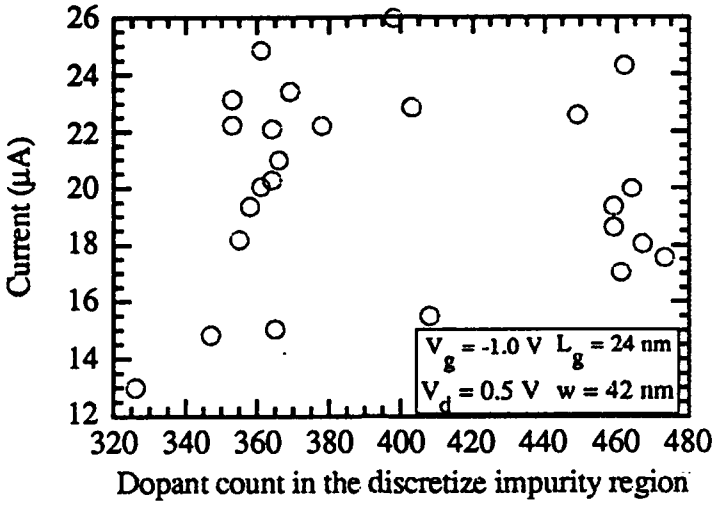

Fig. 3 Current fluctuation versus total dopant in the discretize dopant region.

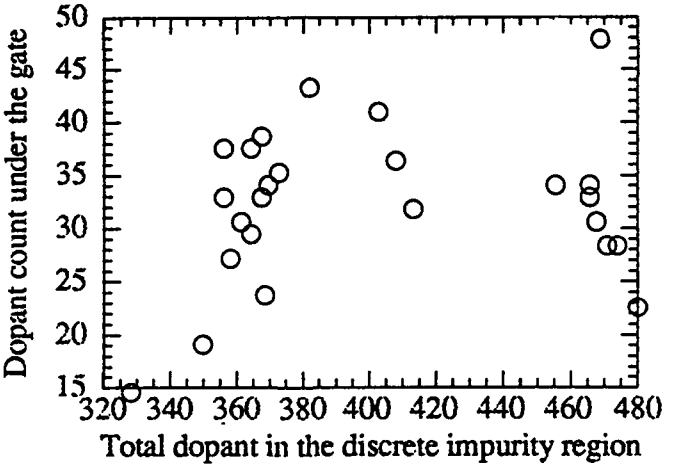

Fig. 4 Dopant number under the gate versus total dopant in the discretize dopant region.

In summary, we have investigated the effect of random impurity fluctuations and distribution on small-device operation. For the device structure simulated here, the results suggest that the effect of random impurity fluctuations and distribution can cause current fluctuation as large as 50 per cent for small MESFET devices if the total gate area is very

small. Further study of different gate length and gate width devices needs to be carried out before more conclusion can be drawn.

References

1. D. K. Ferry, Y. Takagaki and J. R. Zhou, "Future ULSI: Transport Physics in Semiconductor Nanostructures," to be published in Jpn. J. Appl. Phys.

2 J-R. Zhou, and D. K. Ferry, "Simulation of ultra-small GaAs MESFET using quantum moment equations," IEEE Trans. Electron Dev. **39**, 473 (1992).

V. Shubnikov-DeHaas Effect in the Nonlocal Geometry, *Neil Deutscher.* Measurements of the magnetoresistance in a nonlocal geometry can yield information not apparent in conventional local measurements. In a nonlocal geometry the current path and voltage probes are physically separated, which causes the classical resistance to scale as $\exp(-\pi L/W)$ where L is the separation between the current and voltage probes and W is the width of the channel connecting them. This allows effects such as quantum interference, adiabatic transport in edge states and ballistics to dominate the measurement. These effects were thought to scale in terms of the phase coherence length, $\exp(-L/l_\phi)$, but recent experiments have shown this not to be the case.

We are studying the effect of placing a gated region between the current and voltage probes and using it to interfere with the edge channels in high-mobility GaAs/AlGaAs material. We have observed two unusual affects. The preferential measurement of certain SdH peaks, for example we observe a peak at the 3->2 plateau transition but not the 2->3 plateau transition, or vice versa depending on the gate voltage, as shown in Fig. 1. We have also observed Aharanov-Bohm like oscillations due to the presence of the gate, which can be seen in Fig. 2.

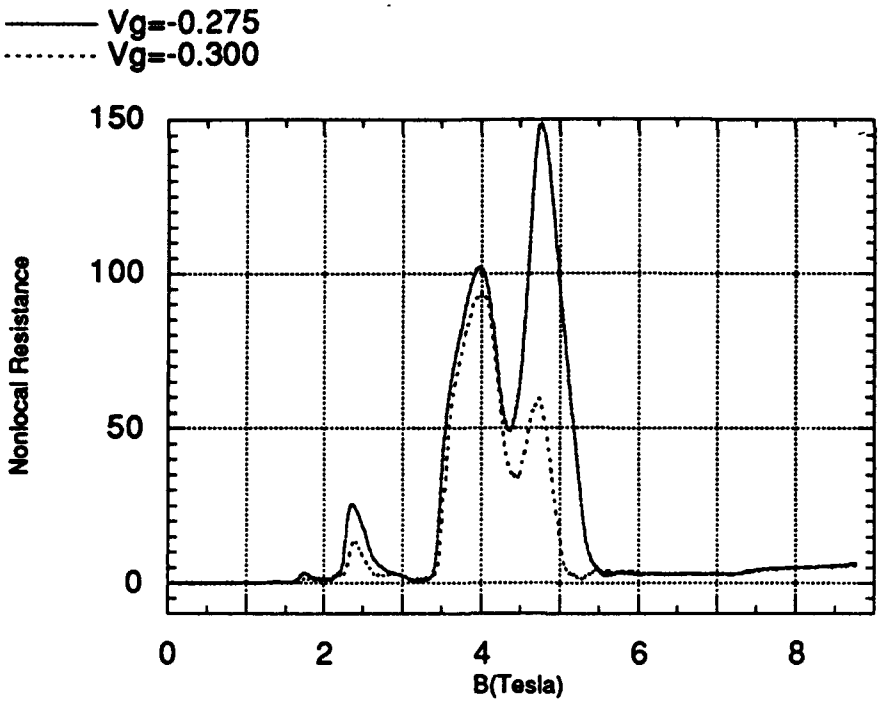

Fig. 1 Variation in relative peak heights with gate voltage.

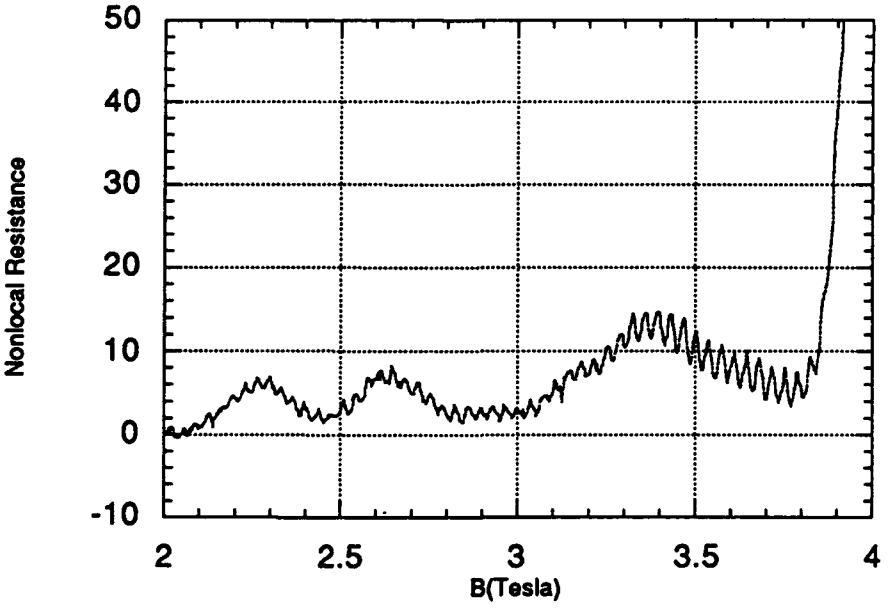

Fig. 2 Aharonov-Bohm oscillations in the nonlocal SdH measurements.